Full dimensional quantum mechanical calculations of the reaction probability of the H + NH 3 collision based on a mixed Jacobi and Radau description

Zhaojun Zhang, Fabien Gatti, Dong Zhang

Full dimensional quantum mechanical calculations of the reaction probability of the H+NH_3 collision based on a mixed Jacobi and Radau description

Zhaojun Zhang[1], Fabien Gatti[2,a)] and Dong H. Zhang[1,b)]
[1]*State Key Laboratory of Molecular Reaction Dynamics and Center for Theoretical and Computational Chemistry, Dalian Institute of Chemical Physics, Chinese Academy of Sciences, Dalian 116023, P.R. China;*
[2]*ISMO, Institut des Sciences Moléculaires d'Orsay - UMR 8214 CNRS/Université Paris-Sud, F-91405 Orsay, France*

The collision between hydrogen and ammonia is a benchmark system to study chemical elementary reactions with five atoms. In this work, we present a description of the system based on mixed Jacobi and Radau coordinates combined with the time-dependent wave packet method to study the H+NH_3 reaction. The Radau coordinates are used to describe the reactive moiety NH_2. A salient feature of this approach is that the present coordinates have the great advantage that a very small number of basis set functions can be used to describe the NH_2 group. Potential-optimized discrete variable representation basis is applied for the vibrational coordinates of the reagent NH_3. The reaction probabilities for several initial vibrational states are presented in this paper. The role of the different vibrational excitations on the reactivity is thoroughly described.

I. INTRODUCTION

Accurate quantum mechanical studies of polyatomic reactive molecular systems are still a great challenge for theoreticians. However, thanks to time-dependent wave packet methods and the rapid growth of the computational power in the past three decades, we can carry out full dimensional calculations for most triatomic and some tetra-atomic reacting systems at a very high level of accuracy.[1–7] However, because of the intrinsic properties of polyatomic reactions, the computational effort growths exponentially with the number of atoms. Therefore, there are still persistent endeavors in the attempts to develop high efficient dynamical methods including the development of potential energy surfaces and of more efficient numerical methods.

It is well-known that, in quantum mechanical simulations, the choice of the coordinates used to describe the molecular system is of great importance. Traditionally, Jacobi coordinates are widely applied in many reactive systems.[8–17] In Jacobi coordinates, for reactions involving three or four atoms, the computational effort may be affordable with modern computers. In addition, the analytical expression of the kinetic energy operator (KEO) in Jacobi coordinates for these reactive systems is relatively simple. However, in some cases, the Jacobi coordinates can create some artificial numerical correlation and lead to the necessity to use large basis sets when solving the Schrödinger equation for the nuclei. Fortunately, for larger systems, i.e. with five atoms or more, some subgroups of the reagents are not strongly altered by the reaction process. Consequently, if the coordinates are well chosen, the computational effort may reduce very significantly. For example, one can fix the coordinates corresponding to the sub-groups that are non-reactive. In this context, it is worth noting that several simulations with methane in reduced dimensionality have been performed.[18–25] In those studies, the non-reactive methyl group was treated as a two dimensional model using a bond length and an umbrella angle forcing the C_{3v} symmetry of the methyl group to be preserved.

H+NH_3 is the simplest five-atomic reaction, which has been widely studied from both experimental and theoretical sides. It is thus an ideal candidate for developing different dynamical methods. In 1997, Corchado and Espinosa-Garcia constructed an analytical potential energy surface (PES) and calculated rate constants with variational transition-state theory.[26] Using the semirigid vibrating rotor target (SVRT) model, Zhang *et. al* carried out a four dimensional calculations for the reaction.[27] The SVRT model can describe the steric effect of the reaction system but neglects some important degree of freedom (DOF) in the reaction system. Yang and Corchado proposed a seven dimensional (7D) model assuming that the nonreactive NH_2 group keeps a C_{2v} symmetry,[28] and that no vibration-rotation coupling exists in the NH_2 group due to symmetry restriction. In 2008, Yang performed for the first time a full dimensional calculation for the title reaction.[29] In this method, three Jacobi vectors were chosen to describe the motion of the NH_3 molecule. He found that the nonreactive NH bonds in NH_3 cannot be treated as a mere spectator, since the three NH bonds are coupled with each other during the reaction process. Thus, we cannot adopt here a reduced dimensional model for this system. Li and Guo reported an accurate global potential energy surface for the H+NH_3 reaction system using permutation-invariant polynomial neural network (PIP-NN) method in 2014.[30] Then Song *et. al* carried out a new calculation based on this PES with the Yang's full dimensional method.[31]

In this paper, we propose a new full dimensional method for reactive systems with five atoms. We use a description based on a successive separation into subsystems with polyspherical coordinates[32], more precisely two Radau vectors and one Jacobi vector for reagent NH_3 and one Jacobi vector for the incoming hydrogen atom. Recently, we have implemented descriptions bases on subsystem coordinates to carry out the full dimensional vibrational and rotational calculations

a)E-mail: fabien.gatti@u-psud.fr
b)E-mail: zhangdh@dicp.ac.cn

for methane and fluoromethane successfully[33,34]: the two subsystems are one atom (one H-atom for CH_4 and the F-atom for fluoromethane) and the remaining CH_3 group. Here, we go one step further by introducing a "subsubsystem" for the NH_2 moiety, which is described by two Radau vectors: the incoming hydrogen atom and NH_3 are the two subsystems and NH_3 is, in turn split into two "subsubsystems", the reactive hydrogen atom and the nonreactive NH_2 moiety. All these groups are described by polyspherical coordinates[32,35,36]. In principle, the polyspherical Radau coordinates are close to the valence internal coordinates and very suitable for the system since the central atom, the N-atom, is heavier than the end atoms, the H-atoms. The kinetic energy operator (KEO) in Radau coordinates is also relatively simple, since the Radau coordinates, like the Jacobi coordinates, are orthogonal coordinates. It is worth noting that, if one of the end atoms is heavier than the central atom, the advantages of using Radau coordinates vanish.

In Ref.[33], we have shown that, if a Jacobi vector joining the center mass of the CH_3 subsystem to the heavy atom, the F-atom, is used combining with a Radau parametrization for the CH_3 subsystem, one can easily calculate the vibrational states of CH_3F. When we study reactive processes, the advantage of combining Jacobi and Radau coordinates will become even more obvious, since the Jacobi coordinates are very convenient to describe bond breaking and creating.

This article is organized as follows. The definition of the coordinates and the corresponding kinetic energy operator (KEO) are given in Section II. Section III presents the time-dependent wave packet (TDWP) method. Section IV presents the results of the method applied to the $H+NH_3 \rightarrow H_2+NH_2$ reaction. A brief summary concludes the article.

II. COORDINATES AND KINETIC ENERGY OPERATOR

In this section, we define the set of coordinates we are using and provide the derivation of the corresponding KEO. The vectors are then parametrized in terms of spherical coordinates and since there are several vectors, they correspond to a particular case of the so-called family of polyspherical coordinates[32,35,36]. While using polyspherical coordinates, it is easy to introduce subsystems[37], i.e. for specific groups of atoms in the molecular system, it is possible to define a Body-Fixed frame and to introduce the spherical coordinates inside this Body-Fixed frame. This introduction of subsystems can be seen as a generalization of the approach for dimers of Brocks *et al.*[38] (see section 2.4 in Ref.[32]). The introduction of subsystems has the advantage that it allows one to introduce coordinates that decouple motions of atoms that are located in very different parts of the molecular system.

Let us consider reaction systems with the structure X+YNZ$_{1,2}$. Fig. 1 gives the combination of Jacobi and Radau vectors we are using. The Radau vectors, $\vec{R}_i$ (i = 1, 2), are the vectors $\overrightarrow{\mathrm{AZ}_i}$ with A the "canonical" point of NZ$_{1,2}$ defined as the geometric mean of NG$_{\mathrm{Z}_{1,2}}$ and G$_{\mathrm{NZ}_{1,2}}$G$_{\mathrm{Z}_{1,2}}$. Here, N refers to the N-atom, G$_{\mathrm{NZ}_{1,2}}$ is the center of mass of NZ$_{1,2}$, G$_{\mathrm{Z}_{1,2}}$ is the center of mass of the Z$_{1,2}$ group. More precisely, the canonical point is defined by $(\mathrm{AG}_{\mathrm{Z}_{1,2}})^2 = \mathrm{G}_{\mathrm{NZ}_{1,2}}\mathrm{G}_{\mathrm{Z}_{1,2}} \times \mathrm{NG}_{\mathrm{Z}_{1,2}}$. If we define $\vec{r}_i = \overrightarrow{\mathrm{G}_{\mathrm{NZ}_{1,2}}\mathrm{Z}_i}$ (i = 1, 2). It entails that

$$\begin{aligned} \vec{R}_1 &= (1-\alpha m_{\mathrm{Z}_1})\vec{r}_1 - \alpha m_{\mathrm{Z}_2}\vec{r}_2 \\ \vec{R}_2 &= -\alpha m_{\mathrm{Z}_1}\vec{r}_1 + (1-\alpha m_{\mathrm{Z}_2})\vec{r}_2 \end{aligned} \tag{1}$$

with

$$\alpha = (1-\sqrt{\frac{M}{m_N}})/m_{\mathrm{Z}_{1,2}}\,, \tag{2}$$

and $m_{\mathrm{Z}_{1,2}} = m_{\mathrm{Z}_1} + m_{\mathrm{Z}_2}$, $M = m_{\mathrm{N}} + m_{\mathrm{Z}_{1,2}}$.

Here we define two subsystems : X and YNZ$_{1,2}$, one Jacobi vector joining X to the center of mass of YNZ$_{1,2}$: this separation is natural since before reaction the X-atom is completely independent form the other part of the system. Now, YNZ$_{1,2}$ is, in turn, split into two subsystems (or "subsubsystems"): the Y-atom and NZ$_{1,2}$. The reason is that we want to describe the breaking of the Y-N bond and the possibility to create a X-Y molecule without introducing too much artificial correlation. Thus, we keep the independence of the NZ$_{1,2}$ subgroup, which will not react with the X-atom.

Thus, NZ$_{1,2}$ has its own Body-fixed frame, BF$_s$. The origin of BF$_s$ is the center of mass of NZ$_{1,2}$ with the z^{BF_s} axis parallel to $\vec{R}_2$. This means that Z$_2$ is on the z^{BF_s} axis. The ($x^{BF_s}z^{BF_s}$) with $x^{BF_s} > 0$ half plane is parallel to $\vec{R}_1$. This means that Z$_1$ is in the ($x^{BF_s}z^{BF_s}$) with $x^{BF_s} > 0$ half plane. The internal vibration of NZ$_{1,2}$ is described by three spherical coordinates: R$_2$, R$_1$, θ. The orientation of the BF$_s$ frame will be parametrized by three Euler angles, α_s, β_s and γ_s, with respect to the Body-Fixed frame of YNZ$_{1,2}$.

YNZ$_{1,2}$ is also treated as a subsystem and has thus its own Body-Fixed frame, BF$_{YNZ_{1,2}}$. The origin of BF$_{YNZ_{1,2}}$ is the center of mass of YNZ$_{1,2}$ with the z$^{BF_{YNZ_{1,2}}}$ axis parallel to $\vec{R}_{NY}$. This means that atom Y is on the z$^{BF_{YNZ_{1,2}}}$ axis. The ($x^{BF_{YNZ_{1,2}}}z^{BF_{YNZ_{1,2}}}$) with $x^{BF_{YNZ_{1,2}}} > 0$ half plane is parallel to $\vec{R}_2$. This means that Z$_2$ is in the ($x^{BF_{YNZ_{1,2}}}z^{BF_{YNZ_{1,2}}}$) with $x^{BF_{YNZ_{1,2}}} > 0$ half plane.

The global Body-Fixed frame, BF, is defined as follows: the origin is the center of mass of the whole system (X+YNZ$_{1,2}$), z^{BF} axis is parallel to $\vec{R}$. This means that atom X is on the z^{BF} axis. The (x^{BF}, z^{BF}) with $x^{BF} > 0$ plane is parallel to $\overrightarrow{NY}$. In other words, atom Y is in the (x^{BF}, z^{BF}) with $x^{BF} > 0$ plane. The orientation of the BF frame is parametrized by three Euler angles α, β, γ with respect to the Laboratory-Fixed (LF) frame.

The BF$_{YNZ_{1,2}}$ frame is oriented by three Euler angles with respect to the BF frame, α_Y, β_Y, γ_Y. α_Y, β_Y are the spherical coordinates of $\vec{R}_{NY}$. The orientation of the BF$_s$ is parametrized by three Euler angles α_s, β_s and γ_s with respect to the BF$_{YNZ_{1,2}}$ frame. α_s, β_s are the spherical coordinates of $\vec{R}_2$ in the BF$_{YNZ_{1,2}}$ frame. In fact, α_s is γ_Y: the first Euler angle of BF$_s$ is the third Euler angle of BF$_{YNZ_{1,2}}$.

The Jacobi vector $\vec{R}_3$ is from the center mass of NZ$_{1,2}$ to atom Y, and $\vec{R}$ is from center mass to atom X. Thus the hamiltonian of the reactant X+YNZ$_{1,2}$ can be writen as (we take $\hbar = 1$):

$$\begin{aligned} \hat{H} = &-\frac{1}{2\mu_R}\frac{\partial^2}{\partial R^2} + \frac{(\vec{J}^{\dagger}_{tot} - \vec{L}^{\dagger}_{YNZ_{1,2}})\cdot(\vec{J}_{tot} - \vec{L}_{YNZ_{1,2}})}{2\mu_R R^2} \\ &- \frac{1}{2\mu_{R_3}}\frac{\partial^2}{\partial {R_3}^2} + \frac{(\vec{L}^{\dagger}_{YNZ_{1,2}} - \vec{L}^{\dagger}_{NZ_{1,2}})\cdot(\vec{L}_{YNZ_{1,2}} - \vec{L}_{NZ_{1,2}})}{2\mu_{R_3}R_3^2} \\ &+ \hat{T}_{NZ_{1,2}} \\ &+ V(R, \beta_Y, \alpha_s, R_3, \beta_s, \gamma_s, R_1, R_2, \theta)\,, \end{aligned} \tag{3}$$

in which

$$\mu_R = \frac{m_X m_{YNZ_{1,2}}}{m_X + m_N + m_Y + m_{Z_1} + m_{Z_2}}, \tag{4}$$

$$\mu_{R_3} = \frac{m_Y m_{NZ_{1,2}}}{m_Y + m_N + m_{Z_1} + m_{Z_2}}. \tag{5}$$

and $\vec{J}_{tot}$ is the total angular momentum operator of the system, $\vec{L}_{YNZ_{1,2}}$ and $\vec{L}_{NZ_{1,2}}$ are the rotational angular momentum operator of the YNZ$_{1,2}$ and NZ$_{1,2}$, respectively. V denotes the potential energy surface.

If we define $u = \cos\theta$ and $u_{\beta s} = \cos\beta_s$ in the following, the integral volume element will be in the following form:

$$dV = dR_1\, dR_2\, du d\alpha_s\, du_{\beta s}\, d\gamma_s\, dR_3\, \sin\beta_Y\, d\beta_Y\, dR\,. \tag{6}$$

In order to obtain the operator $\vec{L}_{YNZ_{1,2}}$, we need expression of the projections of in terms of the angles. The general properties and expressions of the projections of the angular momenta within the framework of the polyspherical approach have been given elsewhere, we just mention here that the BF$_s$

projections for the $\vec{L}_{NZ_{1,2}}$ are given by

$$\begin{bmatrix} L_{NZ_{1,2}\,x^{BF_s}} \\ L_{NZ_{1,2}\,y^{BF_s}} \\ L_{NZ_{1,2}\,z^{BF_s}} \end{bmatrix} = \begin{bmatrix} -\frac{\cos\gamma_s}{\sin\beta_s} & \sin\gamma_s & \cot\beta_s\,\cos\gamma_s \\ \frac{\sin\gamma_s}{\sin\beta_s} & \cos\gamma_s & -\cot\beta_s\,\sin\gamma_s \\ 0 & 0 & 1 \end{bmatrix} \times \begin{bmatrix} \frac{1}{i}\frac{\partial}{\partial\alpha_s} = L_{YNZ_{1,2}\,z} \\ \frac{1}{i}\frac{\partial}{\partial\beta_s} \\ \frac{1}{i}\frac{\partial}{\partial\gamma_s} \end{bmatrix}, \quad (7)$$

and the BF projections are obtained by applying a rotation matrix,$\mathcal{R}(\gamma,\beta_s,\gamma_s)$, to the BF$_s$ components:

$$\begin{bmatrix} L_{\mathrm{NZ}_{1,2}x^{BF}} \\ L_{\mathrm{NZ}_{1,2}y^{BF}} \\ L_{\mathrm{NZ}_{1,2}z^{BF}} \end{bmatrix} = \mathcal{R}(\beta,\gamma) \begin{bmatrix} L_{\mathrm{NZ}_{1,2}x^{BF_s}} \\ L_{\mathrm{NZ}_{1,2}y^{BF_s}} \\ L_{\mathrm{NZ}_{1,2}z^{BF_s}} \end{bmatrix}, \quad (8)$$

with

$$\begin{aligned}\mathcal{R}(\gamma,\beta_s,\gamma_s) &= D_z(\gamma)\times D_y(\beta_s)\times D_z(\gamma_s)\\ &= \begin{bmatrix}\cos\gamma & -\sin\gamma & 0\\ \sin\gamma & \cos\gamma & 0\\ 0 & 0 & 1\end{bmatrix}\times\begin{bmatrix}\cos\beta_s & 0 & \sin\beta_s\\ 0 & 1 & 0\\ -\sin\beta_s & 0 & \cos\beta_s\end{bmatrix},\\ &\times\begin{bmatrix}\cos\gamma_s & -\sin\gamma_s & 0\\ \sin\gamma_s & \cos\gamma_s & 0\\ 0 & 0 & 1\end{bmatrix}\end{aligned} \quad (9)$$

and $L_{YNZ_{1,2}z} = -\frac{1}{i}\frac{\partial}{\partial\gamma}$, $p_{u_{\beta_s}} = i\frac{1}{\sin\beta_s}\frac{\partial}{\partial\beta_s}$ and $p_{\gamma_s} = -i\frac{\partial}{\partial\gamma_s}$.

Now the operator $\vec{L}_{NZ_{1,2}}$ can be obtained

$$\begin{aligned} L_{NZ_{1,2}\,x^{BF}} &= -\cot\beta_s L_{YNZ_{1,2}\,z} + \frac{1}{\sin\beta_s}p_{\gamma_s}\\ L_{NZ_{1,2}\,y^{BF}} &= -\sin\beta_s p_{u_{\beta_s}}\\ L_{NZ_{1,2}\,z^{BF}} &= L_{YNZ_{1,2}\,z}\end{aligned} \quad (10)$$

The term $\frac{(\vec{L}^{\dagger}_{YNZ_{1,2}}-\vec{L}^{\dagger}_{NZ_{1,2}})\cdot(\vec{L}_{YNZ_{1,2}}-\vec{L}_{NZ_{1,2}})}{\mu_{R_3}R_3^2}$ can be calculated in the operator:

$$\begin{aligned}&\frac{(\vec{L}^{\dagger}_{YNZ_{1,2}}-\vec{L}^{\dagger}_{NZ_{1,2}})\cdot(\vec{L}_{YNZ_{1,2}}-\vec{L}_{NZ_{1,2}})}{\mu_{R_3}R_3^2}\\ &= \frac{1}{\mu_{R_3}R_3^2}(\vec{L}^2_{YNZ_{1,2}} + \frac{L^2_{YNZ_{1,2}\,z}}{\sin^2\beta_s}\\ &+ \frac{p^2_{\gamma_s}}{\sin^2\beta_s} + p_{u_{\beta_s}}\sin^2\beta_s p_{u_{\beta_s}}\\ &- 2p_{\gamma_s}L_{YNZ_{1,2}\,z}\frac{\cos\beta_s}{\sin^2\beta_s}\\ &+ \cot\beta_s(L_{YNZ_{1,2}\,z}L_{YNZ_{1,2}\,x} + L_{YNZ_{1,2}\,x}L_{YNZ_{1,2}\,z})\\ &- 2\frac{L_{YNZ_{1,2}\,x}}{\sin\beta_s}p_{\gamma_s}\\ &+ L_{YNZ_{1,2}\,y}(\sin\beta_s p_{u_{\beta_s}} + p_{u_{\beta_s}}\sin\beta_s) - 2L^2_{YNZ_{1,2}\,z}))\end{aligned}$$

The kinetic operator $\hat{T}_{NZ_{1,2}}$ include three parts

$$\hat{T}_{NZ_{1,2}} = \hat{T}_{vib} + \hat{T}_{rot} + \hat{T}_{cor} \quad (11)$$

with $\hat{T}_{vib}$ being the vibrational part of NZ$_{1,2}$, $\hat{T}_{rot}$ being the rotational part of NZ$_{1,2}$, and $\hat{T}_{corr}$ being the coupling between rotation and vibration in the NZ$_{1,2}$.

We just simply give the explicit for the three part the term $\hat{T}_{NZ_{1,2}}$ as follows

$$2\hat{T}_{vib} = -\sum_{i=1,2}\frac{1}{\mu_i}\frac{\partial^2}{\partial R_i^2} - (\frac{1}{\mu_1 R_1^2}+\frac{1}{\mu_2 R_2^2})\frac{\partial}{\partial u}v^2\frac{\partial}{\partial u} \quad (12)$$

where $\mu_1 = m_{Z_1}$, $\mu_2 = m_{Z_2}$, u = cos θ and v = sin θ.

$$\begin{aligned}2\hat{T}_{rot} &= p^2_{\gamma_s}(\frac{1}{\mu_1 R_1^2\sin^2\theta}+\frac{\cot^2\theta}{\mu_2 R_2^2})\\ &+ \frac{1}{\mu_2 R_2^2}(\frac{L^2_{NH3z^{BF_s}}}{\sin^2\beta_s}+\frac{p^2_{\gamma_s}}{\sin^2\beta_s}\\ &- 2L_{NH3z^{BF_s}}p_{\gamma_s}\frac{\cos\beta_s}{\sin^2\beta_s} + p_{u_{\beta_s}}\sin^2\beta_s p_{u_{\beta_s}}) - \frac{p^2_{\gamma_s}}{\mu_2 R_2^2}\\ &+ \frac{\cot\theta}{\mu_2 R_2^2}(-\frac{L_{NH3z^{BF_s}}}{\sin\beta_s}(p_{\gamma_s}\cos\gamma_s + \cos\gamma_s p_{\gamma_s})\\ &- p_{\gamma_s}\sin\gamma_s\sin\beta_s p_{u_{\beta_s}} - \sin\gamma_s p_{\gamma_s}p_{u_{\beta_s}}\sin\beta_s\\ &+ 2\cot\beta_s p_{\gamma_s}\cos\gamma_s p_{\gamma_s})\end{aligned} \quad (13)$$

$$\begin{aligned}2\hat{T}_{cor} &= L_{NH3z^{BF_s}}\frac{\sin\gamma_s}{\sin\beta_s\mu_2 R_2^2}(\sin\theta p_u + p_u\sin\theta)\\ &- \frac{\cos\gamma_s}{\mu_2 R_2^2}(p_{u_{\beta_s}}\sin\beta_s\sin\theta p_u + \sin\beta_s p_{u_{\beta_s}}p_u\sin\theta)\\ &- \frac{\cot\beta_s}{\mu_2 R_2^2}(p_{\gamma_s}\sin\gamma_s\sin\theta p_u + \sin\gamma_s p_{\gamma_s}p_u\sin\theta)\end{aligned} \quad (14)$$

III. WAVEFUNCTION EXPANSION AND TIME-DEPENDENT WAVE PACKET METHOD

The PES used for the scattering calculations in this work was constructed by Li and Guo by using permutation-invariant polynomial neural network (PIP-NN) method fitting to more than 100 000 points at UCCSD(T)-F12a/aug-cc-pVTZ level. More details about the PES can be found in Ref.[30].

To calculate the reaction probabilities, we adopt a time-dependent approach, i.e. we propagate nine-dimensional nuclear wave packets. The time-dependent wavefunction is expanded as

$$\begin{aligned}&\Psi^{J_{tot}MK}_{\nu L}(\vec{R},\vec{R}_3,\vec{R}_1,\vec{R}_2,t) =\\ &\sum_{R,R_3,R_1,R_2,\theta,\beta_s,\gamma_s,L,k,K} F^{J_{tot}MK}_{R,R_1,R_2,R_3,\theta,\beta_s,\gamma_s,L,k}u_n^{\nu_{R_3}}(R)\\ &\times\phi_{\nu_{R_3}}(R_3)\,\phi_{R_1}(R_1)\,\phi_{R_2}(R_2)\,\phi_{\theta}(\theta)\,\phi_{\beta_s}(\beta_s)\,\phi_{\gamma_s}(\gamma_s)\\ &\times Y^{J_{tot}MK}_{Lk}(\vec{R},\vec{R}_3)\end{aligned} \quad (15)$$

where n is a translational basis label, (νL) is the initial rovibrational state of $YNZ_{1,2}$. M and K are the projection of the total angular momentum J_{tot} on the z-axis of space-fixed and body-fixed frames, respectively. k is the projection of the rotational angular momentum L on the z-axis of $YNZ_{1,2}$ frame.

In order to solve the Schrödinger equation, we choose the potential-optimized discrete variable representation (PODVR)[39,40] to compute the matrix elements of the Hamiltonian operator involving $YNZ_{1,2}$. When using PODVR, it is necessary to define a one-dimensional operator to extract the optimized grid points.

For five degree of freedoms "f" (f=$R_1, R_2, R_3, \theta, \beta_s, \gamma_s$), the one-dimensional (1D) reference Hamiltonians are given as follows:

For R_i (i=1, 2, 3),

$$\hat{h}_{R_i} = -\frac{1}{2\mu_i}\frac{\partial^2}{\partial R_i^2} + V_{R_i}^{ref}\,, \tag{16}$$

For θ,

$$\hat{h}_{\theta} = -(\frac{1}{2\mu_1 R_1^2} + \frac{1}{2\mu_2 R_2^2})\frac{\partial}{\partial u}v^2\frac{\partial}{\partial u} + V_{\theta}^{ref}\,, \tag{17}$$

For β_s,

$$\hat{h}_{\beta_s} = (\frac{1}{2\mu_1 R_2^2} + \frac{1}{2\mu_{R_3} R_3^2})p_{u_{\beta s}}\sin^2\beta_s p_{u_{\beta s}} + V_{\beta_s}^{ref}\,, \tag{18}$$

For γ_s,

$$\begin{aligned}\hat{h}_{\gamma_s} =&(\frac{1}{2\mu_{R_3}R_3^2\sin^2\beta_s} + \frac{1}{2\mu_2 R_2^2\sin^2\beta_s}\\ &+ \frac{1}{2\mu_1 R_1^2\sin^2\theta} + \frac{\cot^2\theta}{2\mu_2 R_2^2} - \frac{1}{2\mu_2 R_2^2})p_{\gamma_s}^2\\ &+ \frac{\cot\theta}{\mu_2 R_2^2}\cot\beta_s p_{\gamma_s}\cos\gamma_s p_{\gamma_s} + V_{\gamma_s}^{ref}\end{aligned} \tag{19}$$

In the above 1D Hamiltonians, V^{ref}s are calculated from the total interaction potential with the incoming atom X far away from the reagent $YNZ_{1,2}$ and all other degrees of freedom fixed at the equilibrium value.

The basis set functions for the reactive coordinate, R, are defined as

$$u_n^{\nu_{R_3}}(R) = \begin{cases} \sqrt{\frac{2}{RA}}\sin\frac{n\pi(R-R_0)}{RA} & \nu_{R_3} \le \nu_{asy} \\ \sqrt{\frac{2}{RI}}\sin\frac{n\pi(R-R_0)}{RI} & \nu_{R_3} > \nu_{asy}\,, \end{cases} \tag{20}$$

where RA and RI are the grid ranges of asymptotic and interaction region, respectively. ν_{asy} is chosen to define the basis set that can accurately expand the first several rovibrational states of molecule $YNZ_{1,2}$ far away from X-atom. In other words, the whole space is split into two regions, the asymptotic region and interaction region. In the asymptotic region the interaction between X-atom and molecular $YNZ_{1,2}$ is weak, so we only need a small number of vibrational basis functions for R_3 degree. However, the N-Y bond of the molecular $YNZ_{1,2}$ will break in the interaction region, so more vibrational basis functions are used for R_3. We thus employ different grids in the R coordinate to define the translational basis $u_n^{\nu_{R_3}}(R)$ for different vibrational channels. This is a very efficient way to save the computational effort by dividing the whole reaction process into two parts, and we can easily reduce the vibrational basis for the R_3 coordinate if possible. The reads can find more details in the Ref.[10].

The rotational basis functions for the X+$YNZ_{1,2}$ system in the BF frame is written as

$$Y_{Lk}^{J_{tot}MK}(\vec{R},\vec{R}_3) = \bar{D}_{MK}^{J_{tot}}(\vec{R})\bar{D}_{Kk}^{L}(\vec{R}_3) \tag{21}$$

where $\bar{D}_{MK}^{J}(\vec{R})$ is the Wigner rotation matrix, which depend on the Euler angles that define the BF frame with respect to the Space-Fixed (SF) frame: α, β, γ, and $\bar{D}_{Kk}^{L}(\vec{R}_3)$ is the Wigner rotation matrix, which depend on the Euler angles that define the BF frame of $YNZ_{1,2}$ ($BF_{YNZ_{1,2}}$) with respect to the global BF frame: $\gamma, \beta_Y, \alpha_s$,

$$\bar{D}_{MK}^{J_tot}(\vec{R}) = \sqrt{\frac{2J_{tot}+1}{8\pi^2}}D_{MK}^{*J_{tot}}(\alpha,\beta,\gamma), \tag{22}$$

$$\bar{D}_{Kk}^{L}(\vec{R}_3) = \sqrt{\frac{2L+1}{4\pi}}D_{Kk}^{*L}(0,\beta_Y,\alpha_s). \tag{23}$$

For the specific (J_{tot}, M), a direct product of a localized translational wavepacket $G(R)$ and a specific rovibrational eigenstate $(\nu_0 L_0 K_0)$ for $YNZ_{1,2}$ is chosen to construct the initial wave function,

$$\Psi_{\nu_0 L_0}^{JMK_0}(\vec{R},\vec{R}_3,\vec{R}_1,\vec{R}_2,t=0) = G(R)\psi_{\nu_0 L_0}^{JMK_0}(\vec{R},\vec{R}_3,\vec{R}_1,\vec{R}_2) \tag{24}$$

$\psi_{\nu_0 L_0}^{JMK_0}(\vec{R},\vec{R}_3,\vec{R}_1,\vec{R}_2)$ is the eigenfunction of $YNZ_{1,2}$ which is calculated when the molecular $YNZ_{1,2}$ is far away from the incoming atom X.

The initial wavepacket is propagated using second-order split operator method[41],

$$\Psi(t+\Delta) = e^{-iH_0\Delta/2}e^{-iU\Delta}e^{-iH_0\Delta/2}\Psi(t) \tag{25}$$

where the reference Hamiltonian H_0 is defined as

$$\begin{aligned}H_0 =& -\frac{1}{2\mu_R}\frac{\partial^2}{\partial R^2} + h_{R_3} + \frac{(\vec{J}^{\dagger} - \vec{L}_{YNZ_{1,2}}^{\dagger})\cdot(\vec{J} - \vec{L}_{YNZ_{1,2}})}{2\mu_R R^2}\\ &+ \frac{(\vec{L}_{YNZ_{1,2}}^{\dagger} - \vec{L}_{NZ_{1,2}}^{\dagger})\cdot(\vec{L}_{YNZ_{1,2}} - \vec{L}_{NZ_{1,2}})}{2\mu_{R_3}R_3^2}\\ &+ \hat{T}_{NZ_{1,2}}\end{aligned}$$

and the reference potential U is defined as

$$U = V(\vec{R},\vec{R}_3,\vec{R}_1,\vec{R}_2) - \sum_{i=1}^{3}V_{R_i}^{ref}(R_i) \tag{26}$$

The time-independent wave function ψ_{iE} is calculated using a Fourier transform of time-dependent of the time-dependent wave function as

$$|\psi_{iE}\rangle = \frac{1}{a_i(E)} \int_0^\infty e^{i(E-H)t/\hbar} |\Psi_i(0)\rangle \, dt, \qquad (27)$$

where $a_i(E) = \langle \phi_{iE} | \Psi_i(0) \rangle$ is the overlap between the initial wave packet $\Psi_i(0)$ and the energy-normalized asymptotic scattering function ϕ_{iE}.

The total reaction probabilities for the specific initial state in the whole range of energies can be obtained through calculating the reactive flux at a dividing surface $R_3 = R_{3s}$ as[42]

$$P_i(E) = \frac{\hbar}{\mu_{R_3}} \mathrm{Im}(\langle \psi_{iE} | \psi'_{iE} \rangle)|_{R_3 = R_{3s}}, \qquad (28)$$

where ψ'_{iE} the first derivative of the time-independent wave function in R_3.

IV. APPLICATION AND RESULTS

In this section, we first give a test about the vibrational energy levels of the molecular NH_3 using the combination of one Jacobi and two Radau coordinates. The potential energy surface of NH_3 employed here was constructed by Marquardt *et al.* in 2013.[43] The PODVR and vibrational basis functions are used to extract the vibrational eigenstates.

For radial degree of freedoms R_1, R_2 and R_3, we use 8 vibrational basis functions. For the angle θ, β_s and γ_s, 10, 10, 22 PODVR functions are used, respectively. The parameters used here are much larger than those used for the H+NH_3 reaction. We checked that when the number of the PODVR functions is increased, the vibrational eigenvalues vary very little. Our goal is here to make very accurate calculations with experimental and other theoretical spectroscopic data as a test. But for the calculation of the reaction probabilities, such a high accuracy is not necessary. Thus, the number of PODVR functions here is much larger than for the scattering calculations.

In Table I, the vibrational energies up to the first excitation of the asymmetric stretch excited state are given. In our calculation the tunneling splitting for the first two states is 0.75 cm^{-1}, which is exactly same with the result in Ref 43. Even though in the present method, the three vectors in NH_3 do not have permutation symmetry, the differences between the two theoretical works are negligible, which is the proof of a very high level of convergence. Even for the degenerate states, our method can also provide very accurate results. Generally speaking, our converged results agree very well with the experimental data, validating the present coordinate scheme to calculate vibrational levels of highly symmetric molecules and the reactions involving such molecules.

In the following, we present the full dimensional calculations of the H+NH_3 $\rightarrow$ H_2 + NH_2 reaction. The potential energy surface used here was produced by Li *et al.*[30]. To reduce the size of the basis set, an L-shaped wave function expansion for R and R_3 was used.[10]

A number of 90 grid points is used for R on the range of [1.5,15.0]. 30 grid points are used for the interaction region. For R_3, 30 vibrational basis functions are used in the interaction region and 5 vibrational basis functions are used in the asymptotic region. For R_1, R_2, we use both 3 vibrational basis functions, while 8, 8 and 16 PODVR functions are used for θ, β_s and γ_s coordinates in the NH_3, respectively. For the rotational basis, we use $L_{max} = 30$ and $k_{max} = 3$ and the number of the rotational basis is 205 for $J_{tot} = 0$. Hence the total number of the basis functions used for the reaction reaches $1,700,352,000$ in the interaction region and $566,784,000$ in the asymptotic region, which can provide very well converged results for this reaction, and the memory for the wave functions is about 17 GB in single precision. The center of the initial Gaussian wave packet is located at 13.0 a_0 and the width of the packet is 0.32 a_0.

Because the hydrogen atom exchange channel H'+HNH_2 $\rightarrow$ H+H'NH_2 and abstraction channel H'+HNH_2 $\rightarrow$ H'H+NH_2 exist simultaneously in the reaction, we have to separate them accurately. For our present energy region, the two channels can be easily separated through the distribution of the total reaction probabilies in R grids. In this paper, we only show the results of the abstraction reaction channel and the reaction probabilities were calculated at dividing surface R_{3s}=3.5 Bohr. The vibrational energies for the initial state selected scattering calculations are listed in table II.

The $J_{tot} = 0$ probabilities for the NH_3 two ground states (00^+00) and (00^-00) and their first excited states (01^+00) and (01^-00) are shown in the Fig. 2 and the translational energy is up to 1.2 eV. The curves of the ground states can be considered as a combination of two parts. The first part is the collision energy under about $E = 0.62$ eV, which grows very rapidly and the second part, which energy lies between 0.62 eV and 1.2 eV, increases slower. The reaction probabilities for the (0000) states is very small, about 0.0032 at $E = 1.2$ eV.

Even though there exists a small energy difference between the symmetric and the antisymmetric ground states ((00^+00) and (00^-00)), the probabilities for the two states is exactly the same. Fig. 2b gives the probabilities of the symmetric stretching excitation modes (1000). The threshold energy is very low, about 0.1 eV. The probabilities of the two (1000) states is much larger than for the ground states.

Fig. 3 presents the $J_{tot} = 0$ probabilities for four bending excitation states and four asymmetric stretching excitation states as a function of translational energy. In Fig. 3a we can see the start points of the bending excitation states are about 0.4 eV and the reaction probabilities for this four states is a little larger than the ground states. The differences of the probabilities for the four asymmetric stretching excitation states is much larger than the bending excitation states's in which the probability of $(00^+10)_2$ is about five times larger than the probility of $(00^+10)_1$ as shown in Fig. 3b. It should be noted that our present model cannot provide accurate results for the bending and asymmetric stretching excitation of the reagent NH_3. This is due to the fact that the three bonds of the reactant NH_3 do not have permutation symmetry in our model: these two vibrational modes are both double degenerate, a combination of two degenerate states is also an eigenstate of the system in quantum mechanics. Here, the two eigenstates are not perfectly degenerate with our basis set. However, following the work of Song et al[31], we can obtain the average probabilities of those degenerate states that are also given with a star in the Fig. 3. For the bending excitation states, the average probabilities are agree very well in the whole energy region. For the asymmetric stretching excitation states, the results are essentially the same except a very tiny difference in the high energy region.

In order to display the impact of the different modes on the reaction, we plot the reaction probabilities starting from different excited vibrational states as function of total energy with respect to the energy of the ground state in Fig. 4. The probabilities after excitation of the two stretching modes are the largest almost in the whole energy region, which shows that the excitation of this two modes can greatly enhance the reactivity. The probability of the bending excitation is the smallest when the total energy is about below $E_{tot} = 0.74eV$. The probability of first excitation of the umbrella mode is almost the same as the ground state's which means that the translational energy is more effective than the umbrella exci-

tation on promoting the reaction in the low energy region. The probabilities of the symmetric and asymmetric stretching excitation states are very close especially in the energy region below $E_{tot} < 0.6eV$. Our present result are coherent with the results of Song et al[31] in which the excitation of the two stretching states are nearly equivalent in promoting the reaction.

Finally, we compare our results with those of method based on a pure Jacobi description, i.e. four Jacobi vectors, reported by Song et al using the same PES in 2016.[31]. Fig. 5 depicts the results with the two approaches for the (0000^+) and (1000^+) initial states. For the ground state (0000^+), the two probability curves are almost the same in the whole energy region. For the (1000^+) state, the two results agree with each other very well till the translational energy is about up to 0.6 eV. In the high energy region, the difference is a little larger but still acceptable. As aforementioned, our description in Radau coordinates is more adapted to the fact that the NH_2 moiety is not strongly affected by the process: this is the reason why, we need "only" $1,700,352,000$ basis set functions in the interaction region and $566,784,000$ basis set functions in the asymptotic region to be compared with the $1.45 * 10^{10}$ and $1.6 * 10^9$ basis set functions used by Song et al[44] for the interaction and asymptotic regions, respectively. Thus, we have reduced the size of the basis set by more than eighty-five percent. If one wants to study other five-atomic reactions including heavy atoms like F/Cl+NH_3 which memory consumption may be several dozen to hundreds times larger than for the H+NH_3 reaction, or if we want to add the overall rotation, it is expected that the present Jacobi+Radau approach will be the only one that could treat such reaction systems with affordable computing resources and time consuming along with some parallel acceleration schemes.

V. SUMMARY

A nine dimensional time dependent wave packet study based on a model of the combination of Jacobi and Radau coordinates for the H+NH_3 abstraction reaction has been carried out. The Jacobi vectors were use to describe the bond breaking and the creation of the new chemical bond and the Radau vectors were applied to the nonreactive NH_2 group, which displays no large amplitude motion during the reaction process. The Radau coordinates are adapted when the central atom (here N) is heavier than the other atoms (here the two H atoms). A detail description of the coordinates and KEO were presented as well as the time dependent wave packet method adopted to solve the time-dependent Schrödinger equation. A PODVR grid approach was used for each degree of freedom of reagent NH_3 to reduce the size of the total basis set. Consequently, a relatively small memory was necessary to converge the full-dimensional reactive probabilities. The vibrational energies of NH_3 were also calculated displaying a very good agreement with the result in the literature as well as with the experimental data. We also calculated total reaction probabilities for $J_{tot} = 0$ for several initial vibrational states. Our results show that the probability of the ground state is very small and that the excitation of the stretching modes (symmetric and asymmetric) drastically increase the reactivity. The total energy deposited on the bending excitation mode can not enhance the reactivity in the low energy region, while the stretching excitation modes can increase the reactivity apparently in almost the whole energy region. The probabilities for the ground state and the first symmetric stretching state of our present Jacobi+Radau method and full Jacobi method have shown a very good agreement with each other.

Acknowledgments The project was supported by the National Natural Science Foundation of China (Nos. 21433009, 21688102, and 21703243), the Chinese Academy of Sciences(Grant No. XDB17010000). F.G. thanks "French Chinese Network in Theoretical Chemistry" (GDRI 0808) for financial support.

[1] X. Wang, W. Dong, C. Xiao, L. Che, Z. Ren, D. Dai, X. Wang, P. Casavecchia, X. Yang, B. Jiang, D. Xie, Z. Sun, S.-Y. Lee, D. H. Zhang, H.-J. Werner, and M. H. Alexander, Science. **322**, 573 (2008).
[2] W. Dong, C. Xiao, T. Wang, D. Dai, X. Yang, and D. H. Zhang, Science. **327**, 1501 (2010).
[3] C. Xiao, X. Xu, S. Liu, T. Wang, W. Dong, T. Yang, Z. Sun, D. Dai, X. Xu, D. H. Zhang, and X. Yang, Science. **333**, 440 (2011).
[4] T. Wang, J. Chen, T. Yang, C. Xiao, Z. Sun, L. Huang, D. Dai, X. Yang, and D. H. Zhang, Science. **342**, 1499 (2013).
[5] T. Yang, J. Chen, L. Huang, T. Wang, C. Xiao, Z. Sun, D. Dai, X. Yang, and D. H. Zhang, Science. **347**, 60 (2015).
[6] S. Liu and D. H. Zhang, Chem. Sci. (2015).
[7] D. Yuan, Y. Guan, W. Chen, H. Zhao, S. Yu, C. Luo, Y. Tan, T. Xie, X. Wang, Z. Sun, D. H. Zhang, and X. Yang, Science **362**, 1289 (2018).
[8] R. T. Pack, J. Chem. Phys. **60**, 633 (1974).
[9] G. C. Schatz and A. Kuppermann, J. Chem. Phys. **65**, 4642 (1976).
[10] D. H. Zhang and J. Z. H. Zhang, J. Chem. Phys. **101**, 1146 (1994).
[11] D. H. Zhang and J. C. Light, J. Chem. Phys. **104**, 4544 (1996).
[12] D. Y. Wang, J. Chem. Phys. **123** (2005).
[13] D. Y. Wang, J. Chem. Phys. **124** (2006).
[14] S. Liu, X. Xu, and D. H. Zhang, Theor. Chem. Acc. **131**, 1068 (2012).
[15] J. C. Corchado, J. Espinosa-Garcia, and M. Yang, J. Chem. Phys. **135**, 014303 (2011).
[16] Z. Zhang, T. Liu, B. Fu, X. Yang, and D. H. Zhang, Nat. Commun. **7**, 11953 (2016).
[17] P. Sun, J. Chen, S. Liu, and D. H. Zhang, Chem. Phys. Lett. **706**, 675 (2018).
[18] M. H. Yang, S. Y. Lee, and D. H. Zhang, J. Chem. Phys. **126**, 064303 (2007).
[19] W. Q. Zhang, Y. Zhou, G. R. Wu, Y. P. Lu, H. L. Pan, B. N. Fu, Q. A. Shuai, L. Liu, S. Liu, L. L. Zhang, B. Jiang, D. X. Dai, S. Y. Lee, Z. Xie, B. J. Braams, J. M. Bowman, M. A. Collins, D. H. Zhang, and X. M. Yang, Proc. Natl. Acad. Sci. U.S.A. **107**, 12782 (2010).
[20] R. Liu, H. W. Xiong, and M. H. Yang, J. Chem. Phys. **137**, 174113 (2012).
[21] Z. J. Zhang, Y. Zhou, D. H. Zhang, G. Czako, and J. M. Bowman, J. Phys. Chem. Lett. **3**, 3416 (2012).
[22] Y. Wang, J. Li, L. Chen, Y. Lu, M. Yang, and H. Guo, J. Chem. Phys. **143**, 154307 (2015).
[23] X. Shen, Z. Zhang, and D. H. Zhang, Phys. Chem. Chem. Phys. **17** (2015).
[24] X. Shen, Z. Zhang, and D. H. Zhang, J. Chem. Phys. **144**, 101101 (2016).
[25] Z. Zhao, Z. Zhang, S. Liu, and D. H. Zhang, Nat. Commun. **8**, 14506 (2017).
[26] J. C. Corchado and J. Espinosa-Garcia, J. Chem. Phys. **106**, 4013 (1997).
[27] X. Q. Zhang, Q. Cui, J. Z. H. Zhang, and K. L. Han, J. Chem. Phys. **126** (2007).
[28] M. Yanga and J. C. Corchado, J. Chem. Phys. **126** (2007).
[29] M. Yang, J. Chem. Phys. **129**, 064315 (2008).
[30] J. Li and H. Guo, Phys. Chem. Chem. Phys. **16**, 6753 (2014).
[31] H. Song, M. Yang, and H. Guo, J. Chem. Phys. **145**, 131101 (2016).
[32] F. Gatti and C. Iung, Phys. Rep. **484**, 1 (2009).
[33] Z. Zhao, J. Chen, Z. Zhang, D. H. Zhang, D. Lauvergnat, and F. Gatti, J. Chem. Phys. **144**, 204302 (2016).

[34]Z. Zhao, J. Chen, Z. Zhang, D. H. Zhang, X.-G. Wang, T. CarringtonJr., and F. Gatti, J. Chem. Phys. **148**, 074113 (2018).
[35]F. Gatti, C. Lung, M. Menou, Y. Justum, A. Nauts, and X. Chapuisat, J. Chem. Phys. **108**, 8804 (1998).
[36]F. Gatti, C. Lung, M. Menou, and X. Chapuisat, J. Chem. Phys. **108**, 8821 (1998).
[37]F. Gatti, J. Chem. Phys. **111**, 7225 (1999).
[38]G. Brocks, A. Vanderavoird, B. T. Sutcliffe, and J. Tennyson, Mol. Phys. **50**, 1025 (1983).
[39]J. Echave and D. C. Clary, Chem. Phys. Lett. **190**, 225 (1992).
[40]H. Wei and T. Carrington Jr., J. Chem. Phys. **97**, 3029 (1992).
[41]C. Leforestier, R. H. Bisseling, C. Cerjan, M. D. Feit, R. Friesner, A. Guldenberg, A. Hammerich, G. Jolicard, W. Karrlein, H.-D. Meyer, N. Lipkin, O. Roncero, and R. Kosloff, J. Comp. Phys. **94**, 59 (1991).
[42]D. H. Zhang and J. Z. H. Zhang, J. Chem. Phys. **100**, 2697 (1994).
[43]R. Marquardt, K. Sagui, J. Zheng, W. Thiel, D. Luckhaus, S. Yurchenko, F. Mariotti, and M. Quack, J. Phys. Chem. A. **117**, 7502 (2013).
[44]M. H. Yang, private communication.

TABLE I. Experimental and calculated $L_0 = 0$ levels (in CM^{-1}) for NH_3. Second column: experimental values, third column: calculated values of Ref. 43, fourth column: results with the present approach.

State	Expt.	Reference
(0000)A_1^+	0.00	0.00
(0000)A_2^-	0.79	0.75
(0100)A_1^+	932.43	932.27
(0100)A_2^-	968.12	966.22
(0200)A_1^+	1597.47	1601.46
(0001)E^+	1626.28	1628.45
(0001)E^-	1627.37	1629.33
(0200)A_2^-	1882.18	1878.99
(0200)A_1^+	2384.15	2381.03
(0101)E^+	2540.53	2560.46
(0101)E^-	2586.13	2599.48
(0300)A_2^-	2895.51	2888.81
(0002)A_1^+	3216.10	3220.87
(0002)A_2^-	3217.78	3222.09
(0201)E^+		3222.53
(0002)E^-	3240.44	3246.87
(0002)E^+	3241.62	3248.73
(1000)A_1^+	3336.11	3334.73
(1000)A_2^-	3337.09	3335.61
(0010)E^+	3443.63	3445.85
(0010)E^-	3443.99	3445.99

TABLE II. Vibrational energy (in CM^{-1}) of NH_3 for $L_0 = 0$ calculated on the potential energy surface constructed by li et al.[30]

State	This work
$(00^+00)A_1^+$	0.00
$(00^-00)A_2^-$	0.69
$(01^+00)A_1^+$	940.95
$(01^-00)A_2^-$	972.90
$(0001^+)_1$	1625.41
$(0001^+)_2$	1625.70
$(0001^-)_1$	1625.38
$(0001^-)_2$	1625.67
$(1000)A_1^+$	3331.07
$(1000)A_2^-$	3332.08
$(001^+0)_1$	3437.31
$(001^+0)_2$	3437.63
$(001^-0)_1$	3437.71
$(001^-0)_2$	3438.02

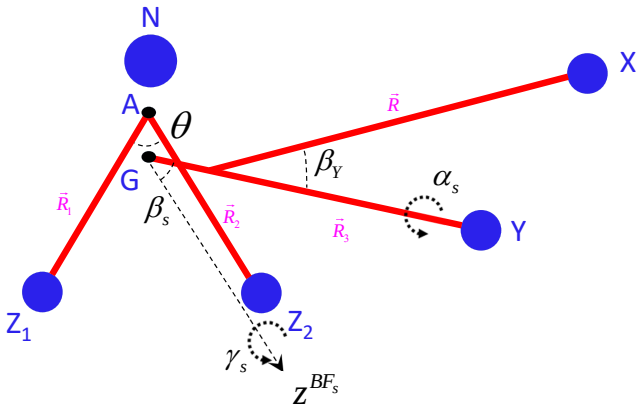

FIG. 1. The Jacobi and Radau vectors for the X+YNZ$_{1,2}$ system. A is the "canonical" point of NZ$_{1,2}$, G point is the center mass of the NZ$_{1,2}$. $\vec{R}_1$ and $\vec{R}_2$ are the Radau vectors. $\vec{R}$ and $\vec{R}_3$ are the Jacobi vectors.

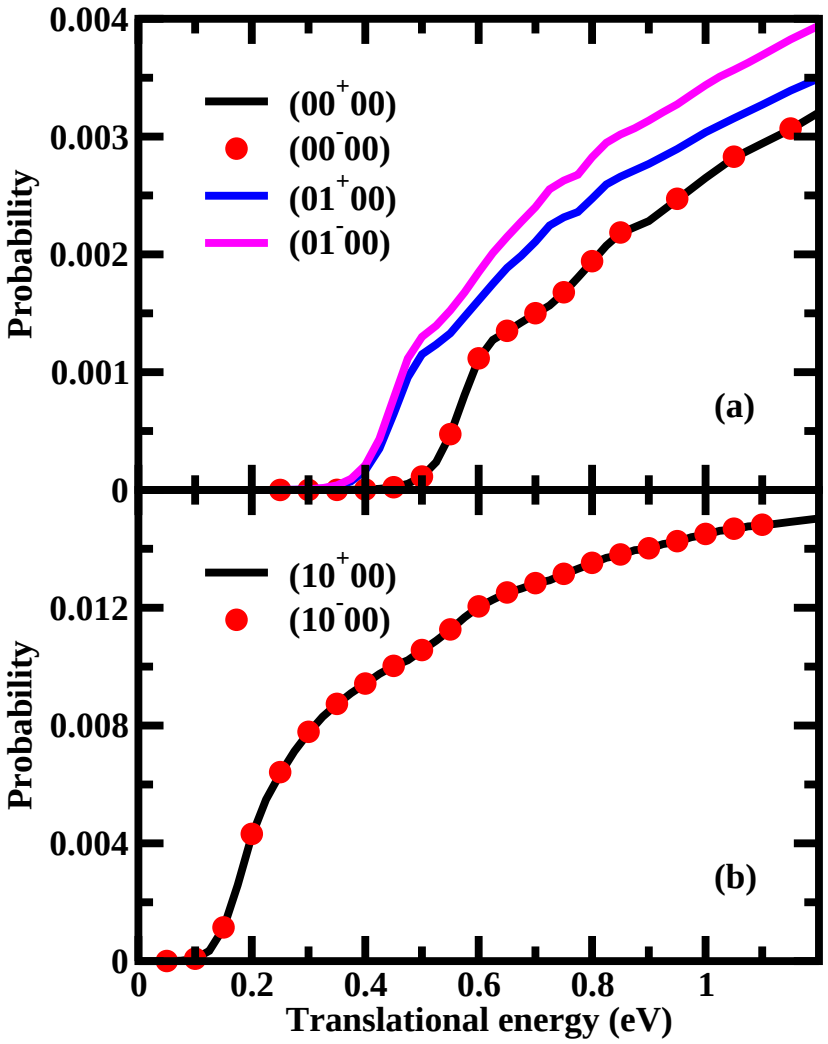

FIG. 2. The $J_{tot} = 0$ total reaction probabilities for the reaction $H + NH_3(\nu_1\nu_2^p\nu_3\nu_4) \rightarrow H_2 + NH_2$ as a function of translational energy. (a) The initial state NH_3 are ground and first umbrella excitation states. (b) Same as (a) but for (1000) states.

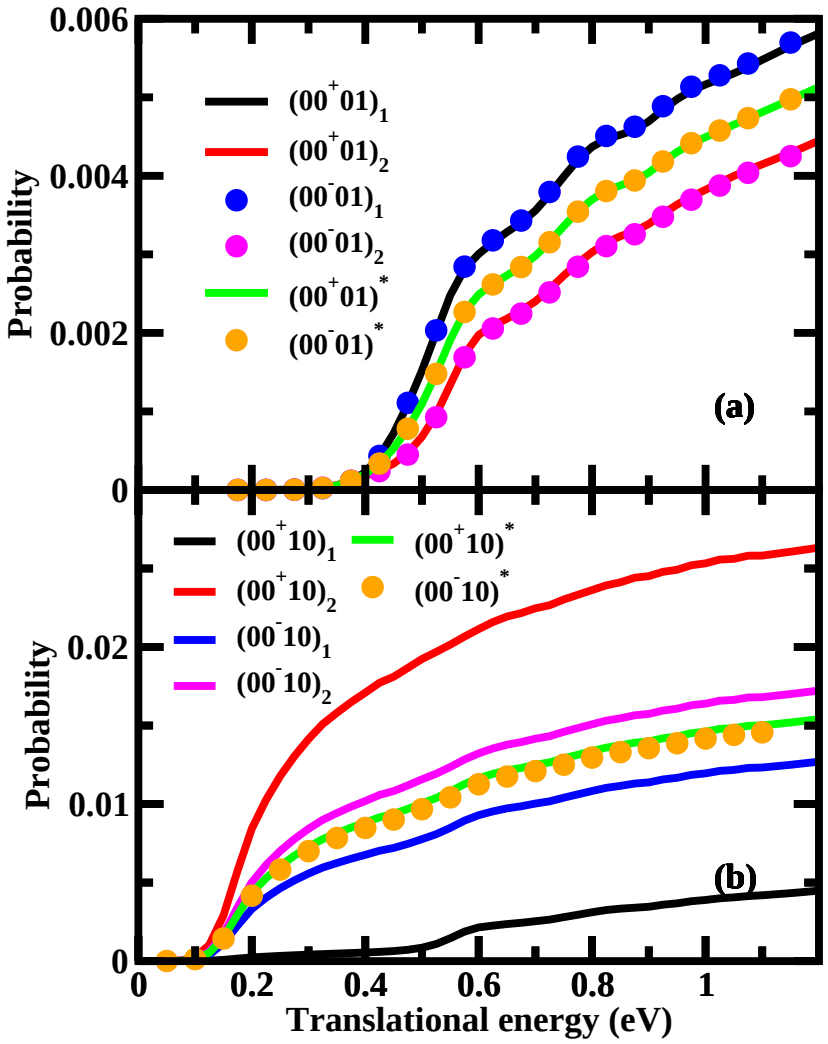

FIG. 3. (a) Same as Fig. 2 but for (0001) states.(b) Same as Fig. 2 but for (0010) states.

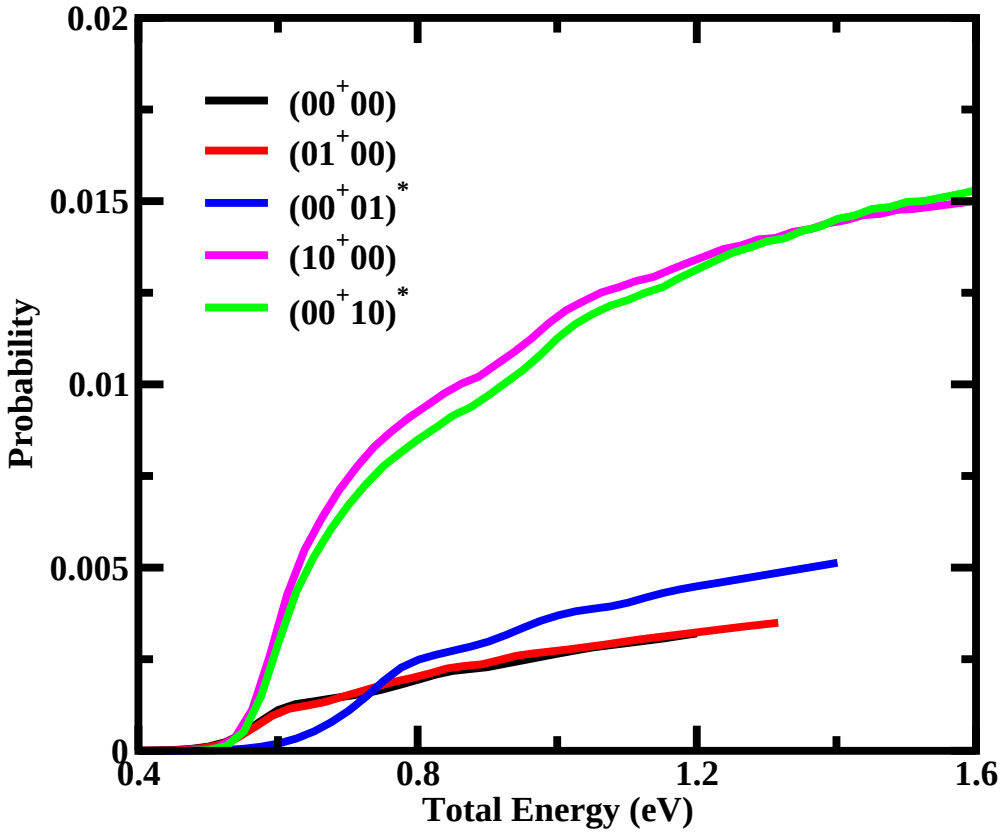

FIG. 4. The J_{tot} total reaction probabilities as a function of total energy measured from the NH_3 ground state (00^+00).

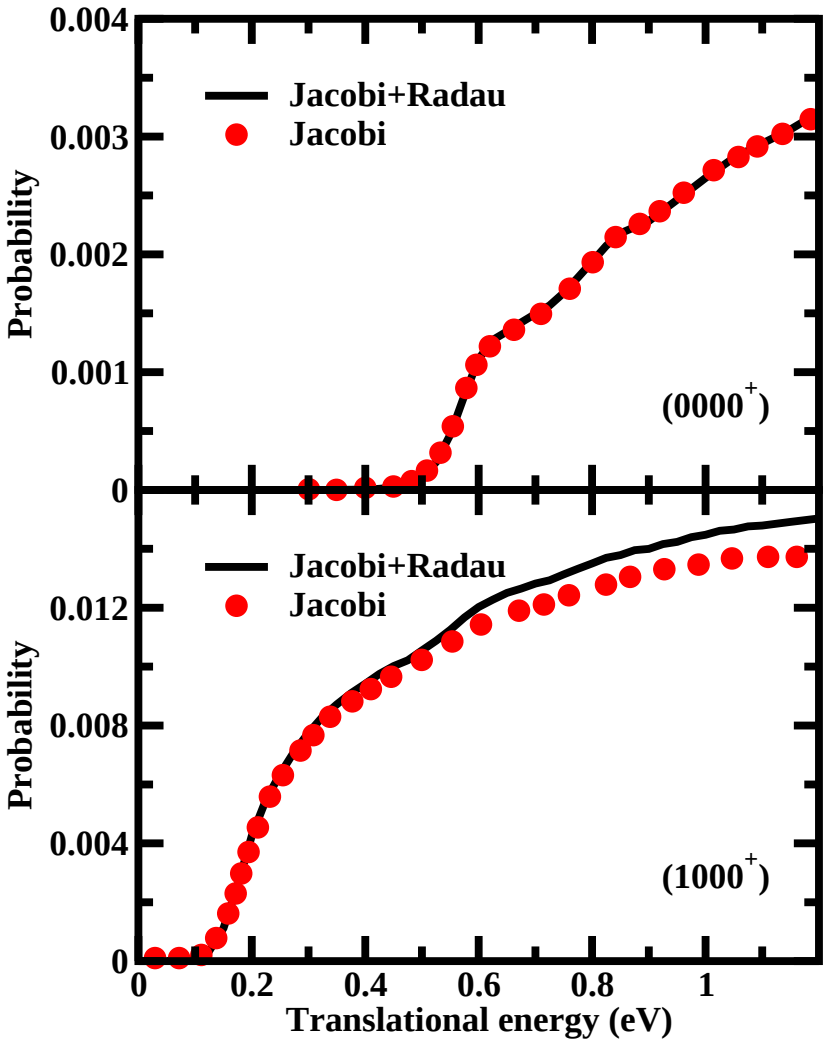

FIG. 5. Comparison of the present (Jacobi+Radau) method and the full Jacobi method for the (0000^+) and (1000^+) initial states.